



HAL
open science

Inter-species variability of root-knot nematode infection dynamics through the simultaneous monitoring of both pathogen and host development

Nathan Jauzion-Graverolle, Claire Caravel, Claude Doussan, Pauline Faubert, Stéphanie Jaubert, Loïc Pagès, Valerie Serra, Suzanne Touzeau, Valentina Baldazzi, Caroline Djian-Caporalino

► To cite this version:

Nathan Jauzion-Graverolle, Claire Caravel, Claude Doussan, Pauline Faubert, Stéphanie Jaubert, et al.. Inter-species variability of root-knot nematode infection dynamics through the simultaneous monitoring of both pathogen and host development. 2025. <hal-05397476>

HAL Id: hal-05397476

<https://hal.inrae.fr/hal-05397476v1>

Preprint submitted on 4 Dec 2025

HAL is a multi-disciplinary open access archive for the deposit and dissemination of scientific research documents, whether they are published or not. The documents may come from teaching and research institutions in France or abroad, or from public or private research centers.

L'archive ouverte pluridisciplinaire HAL, est destinée au dépôt et à la diffusion de documents scientifiques de niveau recherche, publiés ou non, émanant des établissements d'enseignement et de recherche français ou étrangers, des laboratoires publics ou privés.



Distributed under a Creative Commons CC BY-NC 4.0 - Attribution - Non-commercial use - International License

Inter-species variability of root-knot nematode infection dynamics through the simultaneous monitoring of both pathogen and host development

Jauzion-Graverolle N.^{1,4}, Caravel C.¹, Doussan C.³, Faubert P.,¹ Jaubert S.¹, Pagès L.², Serra V.², Touzeau S.^{1,4}, Baldazzi V.^{1*} & Djian-Caporalino C.^{1,*}

¹INRAE, University Côte d'Azur, ISA, Sophia-Antipolis, France

²INRAE, PSH, Avignon, France

³INRAE, EMMAH, Avignon, France

⁴Inria, University Côte d'Azur, MACBES, Sophia-Antipolis, France

* corresponding authors

Abstract

Root-knot nematodes (RKN) cause significant crop yield losses worldwide. However, significant variations in the extent of damage are observed both within and among species. In this study, three economically important plant species in Mediterranean agriculture were selected based on their contrasting susceptibility to RKN infection. Infection dynamics were compared by simultaneously monitoring the development of both the pathogen and the host over two consecutive nematode generations. The resulting data confirmed pronounced differences in symptom expression, particularly during the second cycle. To identify potential sources of the observed variations in host susceptibility, a broad range of functional and architectural plant traits were studied through an integrated experimental-modelling approach. The results suggest that the higher susceptibility of tomato plants may result from the combined effects of reduced photosynthetic capacity and increased hydraulic sensitivity associated with small root diameter. Our results provide new insights into the mechanisms underlying plant tolerance to RKN, offering valuable guidance for plant breeding programs and for designing management strategies that sustain crop productivity while limiting prevent long-term soil infestation.

Introduction

Root-knot nematodes (RKN, *Meloidogyne* spp.) are among the most destructive plant-parasitic nematodes affecting vegetable crops, particularly in the Mediterranean basin. Their ubiquity, extreme polyphagy and ability to parasitise thousands of host species make them a major cause of yield loss in numerous agroecosystems worldwide (Jones et al., 2011, 2013; Wesemael et al., 2011), as they divert nutrients from the plant, leading to its senescence. In Mediterranean vegetable production systems, which are particularly well-suited to RKN establishment (Bernard et al., 2017; Eisenback, 2020), the impact of RKNs has intensified in recent decades (Abd-Elgawad, 2014; Djian-Caporalino et al., 2012; Talavera et al., 2012), affecting nearly half of all cultivated farms. This trend is exacerbated by rising temperatures, which favour faster nematode development, and stricter restrictions on

chemical nematicides (MBTOC, 2006; EC Directive 1107/2009), as well as the broad scale of host-plant availability and specialised, intensive agriculture.

The development feeding sites (galls), which are made up of many hypertrophied endopolyploid cells in the vascular cylinder of the roots, along with atrophy of the tap and lateral roots, are typical belowground signs of RKN infection.(Verdejo-Lucas et al., 2019). As a result, the plant absorbs and translocates less water and nutrients (Shilpa et al., 2022). Plants infected with RKN exhibit aerial symptoms that are comparable to those seen in situations of water scarcity. These include lower fruit quality and quantity, floral abortion, chlorosis and wilting of the oldest leaves, and slowed growth. Senescence and plant death can result from severe infections (Bernard et al., 2017; Chandra et al., 2010; Elnahal et al., 2022; Ortiz et al., 2015).

The number and size of galls (or gall index) are frequently used as a proxy of the severity of the infestation (Xing et al., 2012), while the number of egg-masses is an indicator of RKN reproduction (one female producing one egg-mass that typically contains up to 1000 juveniles in numbers) (Subedi et al., 2020). However, gall size and position within the root system can considerably impact their effect on root function, making gall index a poor indicator of the projected yield loss (López-Gómez et al., 2015, ; Singh, 2013 ; ,Fan et al., 2023). In fact, strong variations in the extent of damages are observed both within and among species, being them susceptible (high gall index leading to strong yield loss or plant death), tolerant (able to sustain a large number of galls) or resistant (no or few galls with no egg-mass) (Seinhorst 1970 ;, Trudgill 1991).

Resistance refers to the ability of the plant to prevent pest development and is conferred by specific genes present only in certain genotypes, whereas for a poor host plant, all species of the genus behave in the same way. This is for example the case of the *Mi1.2* or *Me(s)* gene, present only in resistant tomato and pepper cultivars or rootstocks, respectively (Barbary et al., 2015).. Damage tolerance is independent of resistance and concerns the capacity of a host genotype to grow and maintain an acceptable yield in spite of nematode proliferation. The combination of these two criteria, reproduction and tolerance, form the host status of a plant species or germplasm (Sorribas et al., 2020).

Many physiological mechanisms had been suggested as potentially conferring tolerance, ranging from compensatory mechanisms (increased root growth or nutrient uptake), to change in plant architecture or phenology (delayed senescence, earlier flowering) (Turgill, 1991 ;, Ney et al., 2013). Differences in phenotypic traits, like vessel diameter, canopy architecture or metabolic capacities (reserve remobilisation, carbon reallocation, or secondary exudation) can also be important depending on the considered pest and environmental condition (Ney et a. 2013). Importantly, tolerance is likely to be due to a combination of interacting traits, so that multiple tolerance “strategies” may exist for a same pathogen.

In the case of RKN, root structure and architecture have been suggested as important tolerance traits. The suberin content of the root endodermis has been associated with reduced nematode penetration into the root (Holbein et al., 2019), as well as increased tolerance to water stress conditions, such as the those induced by nematode infection (Baxter, 2009; Maurel et al., 2020). Root system density and depth are known to affect plant water use efficiency (Tron et al., 2015)). Therefore, over-compensatory lateral roots development has been reported in response to nematode attack, as a strategy for plants to mitigate the consequences of nematode infection (Villordon & Clarck, 2018). Consistent with these observations, grafting with resistant rootstocks, selected for their robust root system, has been shown to be a viable technique for managing RKN and reducing plant damages (Okorley et al., 2018). Interestingly, root grafting has been shown to induce systemic changes in many plant processes, including secondary metabolism, photosynthesis and stomatal

conductance (Galvez et al. 2019), suggesting an integrated response to nematode infection that spans multiple regulatory levels.

Thus, deciphering the role of plant physiological processes and phenotypic traits in plant response to RKN requires a system-level and multidisciplinary approach. In this paper, three plant species of economic importance in Mediterranean agriculture were selected based on their differential susceptibility to RKN infection, and used to assess infection progression and outcome.

The objective was twofold. Firstly, the present study provided a unique description of the infection dynamics through the simultaneous monitoring of both pathogen and host development, including phenology and growth of shoots, roots and fruits, over two nematode cycles.

Secondly, we attempted to identify potential sources of the observed variations in plant susceptibility. Unlike most published works, we did not focus on a single putative mechanism, but rather performed an overall screening of a range of plant architectural and functional traits that may play a role in the interaction between plants and nematodes. To do this, we used a combination of multiple techniques ranging from hydraulic measurements, microscopy to functional-structural modelling.

By focusing on interspecific rather than intraspecific differences, we were able to increase the variability of plant traits (e.g. different root system architectures) and explore contrasting qualitative patterns of plant susceptibility. This allowed us to better understand the phenotypic traits that can affect plant susceptibility, either individually or in combination. Our study also highlights culture growing conditions that may limit the expression of potentially tolerant traits. This is the case of cucurbits, which were found to possess a deep root system and a rapid root elongation rate but suffered from pot culture. Ultimately, identifying and deciphering the role of plant tolerant traits is a key challenge for plant breeding, as well as for the design and improvement of control strategies that both maintain the yield and soil infestation in the long-term.

Material & Methods

Plant material

The lines of the 3 plant species, commonly used in Mediterranean cropping systems due to their agronomic interest, were chosen because they exhibit contrasting susceptibility or tolerance to *M. incognita*. Tomato (*Solanum lycopersicon*) cv. Saint Pierre was provided by Vilmorin™ France. Pepper (*Capsicum annuum*) cv. Doux Long des Landes, provided by Inrae Avignon GAFL Unit, was 3 to 5 times less susceptible than tomato Saint Pierre to *M. incognita* (Djian-Caporalino et al., 1999). The hybrid squash root stock (*Cucurbita moschata* X *C. maxima*) cv. TZ 148 F1, provided by Clause™ France, was tolerant to RKN (Delmas & Goillon, 2016).

Nematode rearing for the inoculation

Six 4-week old tomato plants of the cultivar Saint Pierre were inoculated with soil contaminated with the Morelos population of *M. incognita*, obtained from the INRAE collection maintained in Sophia Antipolis (France). They were grown in a greenhouse for 6 weeks, until the roots presented egg masses containing at least 50% of eggs with visible juveniles inside. The plants were then removed from the pots and the roots were carefully cleaned, cut and blended for 1 minute in a 0.5% active chlorine solution to fragment the egg masses and free the eggs from the mucus. The mixture was filtered through several sieves with tap water to remove plant and chlorine residues, then through a

5µm sieve retaining only the eggs. The eggs were washed in a beaker with mineral water and counted with binoculars. Approximately 1,700,000 eggs were obtained.

To obtain the juveniles stage 2 (J2s, the only infective stage) necessary for the root hydraulic experiments, 500,000 eggs were placed on a 10µm sieve in a hatcher made up of a glass box with mineral water and an air bubbling. The larvae were collected from the bottom of the box every 3 days and kept at 15°C until the necessary 50,000 J2s were obtained.

Plant growth and RKN development experiments

For these experiments, 50 seedlings of each species were germinated on wet cotton on a dark room at 25°C for 3 days. They were then planted in small pots filled with a clean potting soil and grown for one week for squash and one month for pepper and tomato in a climate-controlled room. The seedlings were then transplanted into 3 L pots (12 cm deep pots) filled with 2kg of sandy soil (80% sand, 7% loam, 4% clay, 2.8% organic matter) and moved into a greenhouse maintained at a temperature above 18°C for one week to acclimatize them to the new conditions. Fertilization was carried out by drippers in order to maintain a constant, but not excessive, water availability in the substrate. The control plants and the plants to be inoculated were randomly divided into crop groups (3 blocs, one for each crop). The climate was monitored in the greenhouse to ensure that climate conditions were relatively stable. A probe recorded every minute the air temperature in the greenhouse. Cumulative daily degrees ($S = \text{Sum} [T_{\text{max}} - T_{\text{min}}] / 2 - T_b$) for *M. incognita* was recorded each day to determine the completion of each cycle calculated according to Ploeg & Maris (1999) with a base temperature (T_b) and a required heat sum (S) of 10.1°C and 400°C.day respectively. We expect this value to be more than 400 since we inoculate with eggs instead of 2nd stage juveniles.

One day before inoculation, plants were watered up to field capacity and drippers were removed. An inoculation solution was prepared with a concentration of 2700 eggs per mL. 36 plants (12 tomato, 12 peppers and 12 cucurbits) were inoculated by digging in the soil two small trenches, 3cm and 6cm to the stem. In each trench, 4mL of inoculation solution was added two times, in order to mitigate the risk of eggs running off with the water. In total, each plant received about 21600 eggs corresponding to 10 eggs per cm³ of soil. Drip fertirrigation was installed back one day after inoculation and delivered daily 200mL per plant in 2 times during the first cycle and 400mL per plant in 3 times during the second cycle (Electro conductivity of the irrigation water at 1.1 dS/m). Plants were kept 12 weeks until RKN completed 2 life cycles.

Plant related measurements

At the date of the inoculation ($t=0$), 18 non-inoculated plants (6 per crop) were used to have fresh and dry mass data. They were delicately removed from the soil and washed under clear water, weighed, cut and dried in an oven at 80°C for 10 hours, then weighed again. Every week, for each plant, the plant height, the number of leaves, flowers at anthesis, developing fruits and abortions were recorded. At $t+6$ and $t+12$ weeks, the fresh and dry masses of the roots, aerial parts and fruits were measured for both inoculated and control plants.

Nematode related measurements

In order to follow the RKN population dynamics, specific measurements were taken for the inoculated plants. After 6 weeks, equivalent to a full RKN life cycle, roots were removed from the soil and

the number of galls with and without egg masses, egg-masses after eosin staining (1 min in a 4.5g/L solution of eosin B), and number of eggs per egg-mass (mean for 10 egg-masses mixed 1 min in 1mL of 1% sodium hypochlorite) were counted. After 12 weeks (approximately 2 RKN cycles), the gall index (GI) was measured on Zeck scale from 0: “no infestation” to 10: “dead plant” (Zeck, 1971). For peppers and tomatoes, the number of galls with and without egg masses was also counted as it was done at 6 weeks. Finally, the remaining living juveniles (J2) of *M. incognita* in the soil were also identified and counted after extraction of contaminated soil through an Oostenbrink elutriation (Oostenbrink, 1960).

The number of galls and the gall index provide a proxy for infestation severity. The number of egg masses is an indicator of parasitic success and reproduction rate. The reproduction factor (final population/initial population) was calculated using the number of eggs per egg mass x number of egg masses / number of eggs inoculated per plant. The number of free *M. incognita* J2 in the soil at the end of the second cycle complements these data (Sorribas et al., 2020).

Climate-controlled experiment for photosynthesis CO₂ response curves

Six seedlings of each species were germinated on wet cotton in a dark, heated chamber at 24°C for three days. They were then planted in 2 L containers filled with clean potting soil and grown in a climate-controlled room for approximately 5 weeks.

The photosynthetic response of the three species to internal CO₂ level (A-Ci curve) was assessed using a Li-COR 6400 portable systems. The first fully expanded leaf was selected on each plant and exposed to 600 $\mu\text{mol m}^{-2} \text{s}^{-1}$. The block temperature was maintained at 27°C using a flow rate of 500 ml min^{-1} and ambient humidity. They were initially placed in the chamber at 600 p.p.m. CO₂, a value close to the ambient CO₂ concentration. CO₂ was reduced stepwise to 50 p.p.m and then increased again in a stepwise manner until 1800 p.p.m. or photosynthesis saturation, depending on the species. Overall, 8-10 different CO₂ concentration levels were tested on each A-Ci curve. The leaves were maintained for a period of 10 to 20 minutes in each condition in order to ensure that photosynthetic activity had stabilised. Three to five leaves were measured on different plants, for each species.

Root Phenotyping experiments

For the root phenotyping experiment, 18 tubes (1 m long x 100 mm diameter) were filled with a 50/50 mixture of sand and potting peat (Potgrond H90, Klasmann-Deilmann) sieved at 2.5mm. Seeds were sown by direct sowing, to avoid alteration of root architecture at transplanting. One seed of each species was sown in 6 tubes. The plants were grown in a greenhouse and watered with a solution of diluted Liquoplant Rose(3‰). The plants were excavated before reaching the bottom of the tube on 2 dates, depending on the development rate of each species. Excavation was done after saturating the tube under water and then gently washing the roots. For each plant, a 25 cm section of the taproot and a main root are removed with their branches and scanned by transparency at 2400 dpi (Epson V850 scanner). On these images, we measured the apical diameter of each branch from the youngest (on the apex side), its distance from the previous one, as well as the diameter of the mother root lateral insertion. These data were analyzed, together with global measurements

taken during excavation, to calculate root parameters necessary for the Archisimple root architecture model (Pagès et al., 2014).

Root Hydraulic conductivity measurements

A set of 30 tubes (50 cm x 100 mm diameter) was filled with the same 50/50 mix of sand and potting peat, used in the root phenotyping experiment. Seeds were sown in the same substrate in 6.5cm cups and transplanted into 10 tubes per species 3 days before nematode inoculation. Cucurbit roots were pruned at transplant, tomatoes lightly trimmed, peppers left intact. Inoculation of 6 tubes per species with larvae at the J2 stage was carried out in 3 holes distributed around the seedling using a micropipette (approx. 2700 J2/cucurbit tube, 3072 J2/ tomato tube and 1416 J2/ tube for the small peppers). The plants were grown in a greenhouse and watered with a solution of diluted Liquoplant Rose. Three inoculated and two healthy plants per species. were harvested at 2 dates. To investigate the impact of nematodes on water transfer in the root system, two types of root hydraulic conductance measurements were performed: total root system hydraulic conductance and axial conductivity of basal main root segments.

Total root system hydraulic conductance (L_p)

Hydraulic conductance was measured using the 'tension' technique (North and Nobel, 1995) with increasing suctions ($P \sim -0.16, -0.3, -0.5$ bar) imposed to the root basal part by a vacuum pump. For total root system hydraulic conductance (L_p), the tubes containing the root system are immersed in water and the plant cut at the stem base. The cut stem is fitted with a tygon tube to a graduated pipette to determine the flow rate (Q) induced by the suction from vacuum pump. L_{p_tot} (cm³/s/bar) was determined by the slope of the linear regression between Q and P and further normalized by the dry mass of the root system (M) for getting L_p (cm³/bar/s/g): $L_p = Q / (\Delta P \cdot M)$.

However, at higher suctions (i.e. from -0.5 bar), bubbles often appeared, originating from the immersed root system probably from air trapped in tissues. Such air-affected suctions were discarded from calculations.

Axial hydraulic conductivity (K_h)

Axial hydraulic conductivity (K_h) was measured on root segments of about 5 cm length retrieved from basal main roots (4 segments from different plants per treatment and date). Axial conductivity was measured at that basal location because if axial xylem flow in main roots is impeded by nematodes at this place, it would more severely impact the water uptake than distal locations. For plants with nematodes, root segments showing a thickening from nematode infection were selected. About 1 mm of the cut distal end of root is immersed in a 100 mM KCl water while the distal end with cortex removed for about 5 mm is connected to a graduated pipette with ad-hoc tygon tubes fitting between root and pipette. A tight seal at the tube-root junction is done by applying a dental paste (Coltene President, regular body). The same P sequence as above is applied and the corresponding induced flow (Q) recorded from meniscus displacement in the pipette. K_h (m⁴/s/bar) is the slope of the linear regression between Q and P multiplied by the root length (l):

$$K_h = Q / \left(\frac{\Delta P}{l} \right).$$

Root segment diameters were measured near the distal and basal end and a mean cross section area of root estimated.

Statistical analysis

Treatment and species comparison

Non parametric Wilcoxon test has been used to compare differences among species and between treatments (stat_compare_means() function of R ggplot package) Statistical significance is reported according to standard notation * $p \leq 0.05$, ** $p \leq 0.01$, *** $p \leq 0.001$, **** $p \leq 0.000$.

A/C_i curve-fitting

The response of photosynthesis rate to intracellular CO₂ concentration (A/C_i curve) was fitted to the model of Farquhar et al. (1980), following the procedure described in (Long & Benacchi, 2003). Accordingly, the A/C_i curve can be subdivided into two or three phases, depending of the underlying limiting process.

At low CO₂ concentration, photosynthesis depends essentially on the Rubisco activity, modulated by oxygen concentration, and can be described using the following formula

$$A = V_{c,max} \frac{C_i - \Gamma}{C_i + K_c(1 + O/K_o)} - R_d, C_i < C_1^{th}$$

where $V_{c,max}$ is the maximum Rubisco activity and R_d is the photo- respiration rate. Temperature-corrected values for K_c , K_o and Γ were fixed according to Bernacchi et al. (2001)

When further increasing the CO₂ concentration, the A/C_i curve shows an inflection when the RuBP regeneration becomes limiting. The corresponding model reads

$$A = \frac{J C_i}{4 C_i + 8 \Gamma} - R_d, C_1^{th} < C_i < C_2^{th}$$

where J is the whole chain electron transport rate under the current conditions of light and temperature.

In some situations, photosynthesis rate may reach a plateau at high CO₂ concentration, reflecting a limitation for triose-phosphate utilisation. In this regime, the A/C_i curve can be described as:

$$A = 3 V_{TPU} - R_d, C_i > C_2^{th}$$

By imposing continuity of the functions at CO₂ thresholds, J , V_{TPU} can be expressed as functions of the other variables. The two unknown quantities $V_{c,max}$, R_d were estimated using a least-square method (nls function, R programming language), minimizing the agreement between model and data. The fit was repeated for a set of different threshold values C^{th} , ranging from 150 to 1800 $\mu\text{mol mol}^{-1}$. A model selection approach was used to identify the (C_1^{th}, C_2^{th}) pair giving the best fitting to data according to the Aikake Information criterium (Burnham & Anderson, 2002), which penalises over-fitting.

Results

Dynamics of RKN infection shows plant species-specific patterns

The severity and progression of nematode infestation were monitored over a 12-week period, corresponding to two complete *Meloidogyne* spp. developmental cycles under our experimental

conditions. Pronounced differences in the number of galls and egg masses were observed among the three crop species.

During the first cycle, inoculated tomato plants developed the highest number of galls, followed by cucurbits and peppers (Figure 1). In the second cycle, the gall index (Zeck scale) —reflecting both the number and size of galls—increased markedly in cucurbits, surpassing that of tomato plants, while peppers maintained consistently lower values. Despite the resurgence of infection after two nematode generations, pepper plants remained only moderately affected, with an average gall index of 3, compared to 6 for tomato and 7.5 for cucurbits. Cucurbit root systems were the most severely compromised, displaying extensive thick galls, and a marked reduction in the formation of fine young roots. Tomato roots also exhibited large, thick galls and a lower proportion of young roots, with most of the roots being lignified. In contrast, pepper roots showed numerous small galls but few large ones, and the primary symptom observed was a moderate reduction in overall root system size

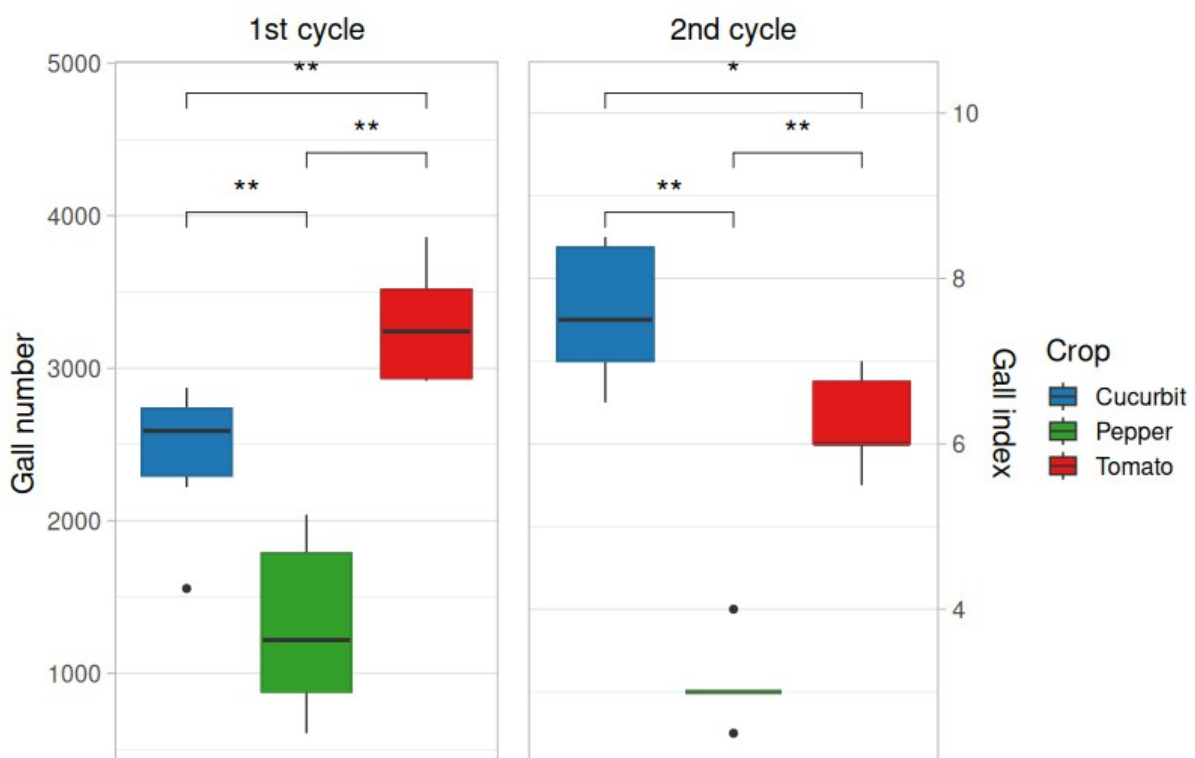


Figure 1: Nematode infestation severity for the three species after one or two RKN cycles (Pairwise comparisons, Wilcox test, n=6).

After one nematode cycle, tomato plants exhibited more than twice the number of visible egg masses compared with pepper and cucurbits, indicating rapid *Meloidogyne incognita* establishment and development, consistent with their status as a good host (Figure 2). Correspondingly, the reproduction factor (calculated as the number of eggs per egg mass × number of egg masses / initial eggs inoculated per plant) was significantly higher in tomato than in the other crops ($p < 0.01$), whereas female fecundity (eggs per egg mass) did not differ significantly among the host species.

During the second cycle, infection dynamics diverged among the three species. In tomato, the number of egg masses, eggs per egg mass, and Pf/Pi decreased relative to the first cycle, suggesting a

progressive slowdown in nematode reproduction. Conversely, pepper plants exhibited accelerated infection, with a threefold increase in both egg mass number and Pf/Pi. In cucurbits, the number of egg masses could not be determined due to the excessively high gall index; however, the number of eggs per egg mass remained stable in both pepper and cucurbits (data not shown).

At the end of the experiment, the density of *M. incognita* juveniles remaining in the soil corroborated the higher infestation levels in tomato and cucurbit soils compared with pepper (Figure 3).

Free-living saprophagous nematodes (at all stages), also extracted from the soil and counted, were 5 to 10 times less abundant in pepper culture than in cucurbit and tomato pots, respectively (Figure 3).

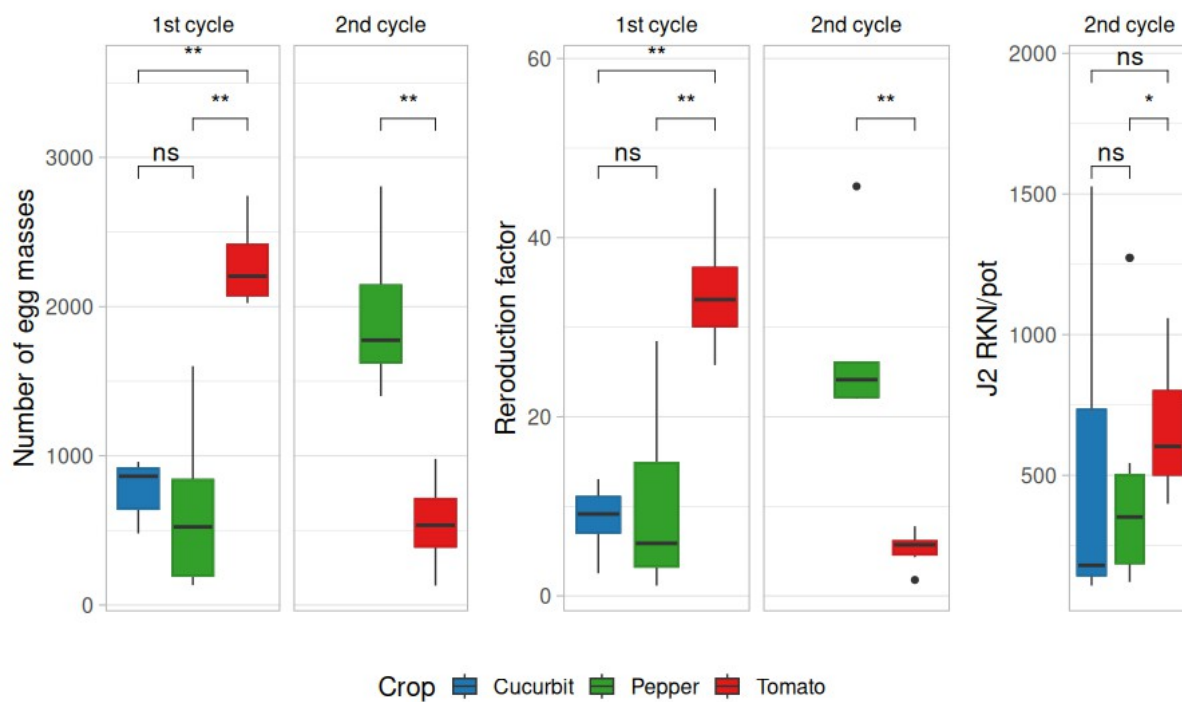


Figure 2: Nematode infection for the three species after one or two RKN cycles (Pairwise comparisons, Wilcox test, $n=6$). The indicators are the number of egg masses per plant, the reproduction factor Pf/Pi (eggs per egg mass \times number of egg masses / eggs inoculated per plant) and the average number of free living RKN (j2) remaining in the pots of 2L of soil after an Oostenbrink elutriation .

Plant growth and phenology under nematode infection

Plant growth and development were monitored throughout the course of nematode infection to assess how the three species coped with *M. incognita*. Weekly measurements included plant height, number of leaves, number of flowers, and number of fruits for both inoculated and control plants. The impact of nematode infection became apparent at the onset of the second life cycle and intensified as the experiment progressed (Figures 3). In tomato and cucurbits, plant growth was reduced, leaf number declined, and fruit set was delayed by approximately one week.

After a single nematode life cycle, i.e., six weeks after inoculation (WAI), fresh and dry biomass of roots and aerial parts generally did not differ significantly between inoculated and control plants for any of the species studied (Figures 4). An exception was observed for pepper roots, where dry mass was 2.5 times higher in control plants compared with inoculated ones; however, this difference was not reflected in the corresponding fresh mass, suggesting a possible artifact during sample drying.

At the end of the experiment, after two nematode life cycles (12 WAI), tomato and cucurbit plants exhibited approximately a 50% reduction in aboveground dry mass and leaf number relative to control plants. For all species, root system dry mass of inoculated plants was higher due to gall formation, which confounds interpretation, making root mass an unreliable indicator of plant development.

In contrast, pepper plants demonstrated a high level of tolerance to root-knot nematode infection. Despite the accelerated infection dynamics, plant growth remained largely unaffected (Figure 3), and no significant reductions in aboveground dry mass or yield were observed after two nematode life cycles (Figures 4).

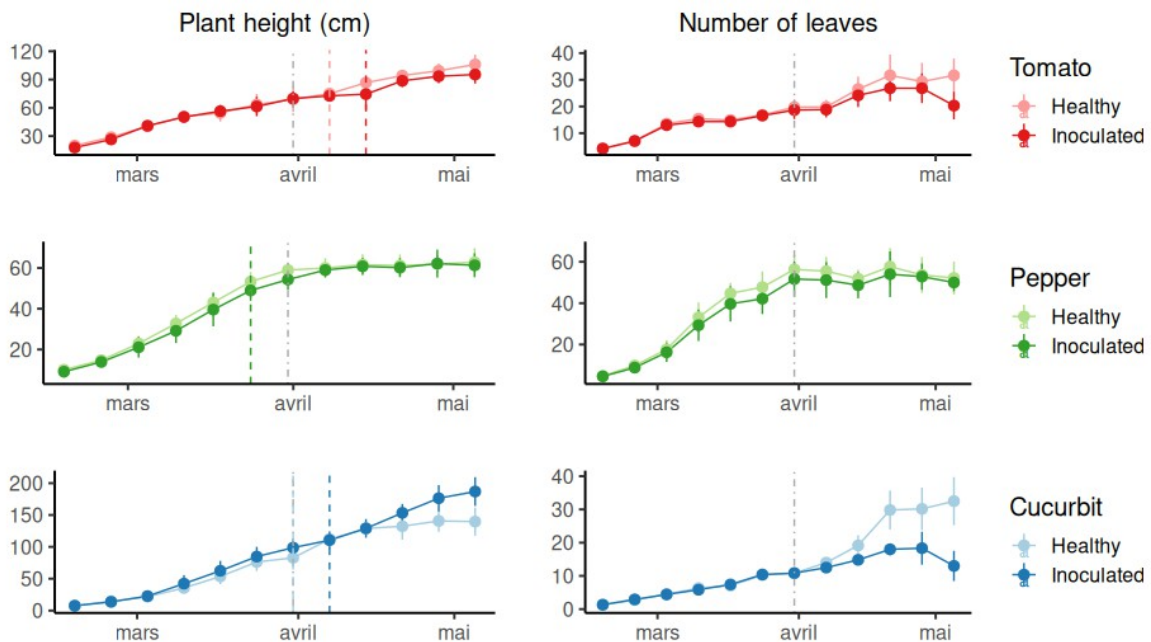


Figure 3: Dynamics of plant growth and leaf emission, for the 3 species. Colored dashed lines indicate the time of first fruit set for control and inoculated plants. The grey dot-dashed line indicates the onset of the second cycle.

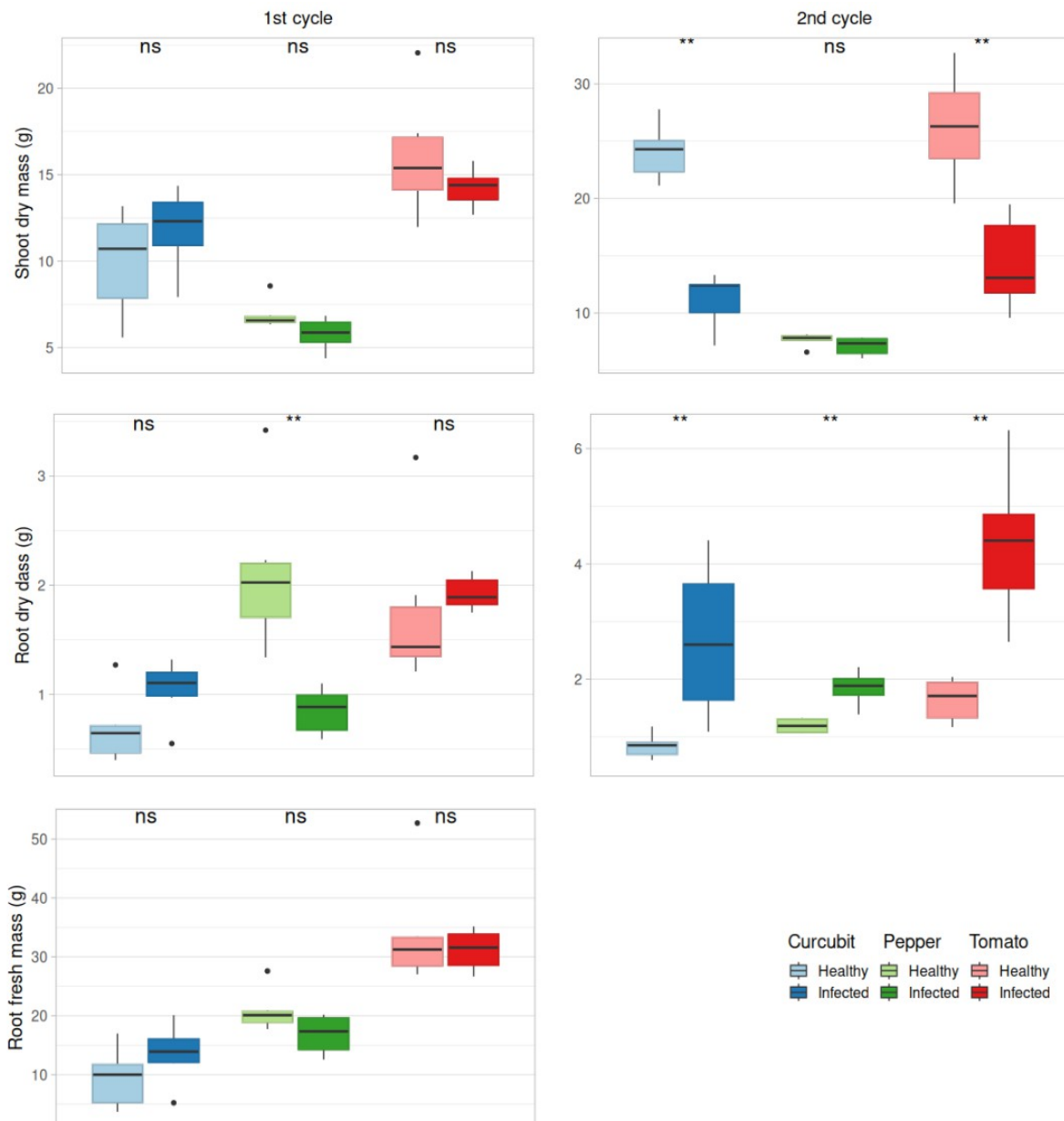


Figure 4: Fresh and dry masses of tomato cv. *St Pierre*, pepper cv. *DLL* and cucurbit rootstock cv. *TZ 148* after one or two RKN cycles (6 or 12 weeks after inoculation, respectively). Plants were inoculated with 21600 *M. incognita* eggs and compared to controls free of RKN. Asterisks indicate statistical significance between controls and inoculated plants (Wilcox test, $n=6$).

The three species display distinct root system architectures

The root system constitutes the primary interface between plants and soil-dwelling nematodes, determining both the opportunity for *M. incognita* to locate and invade new roots and the plant's capacity to withstand root deformation and water stress induced by infection. To elucidate the contribution of root system architecture (RSA) to the observed infection dynamics, a

dedicated phenotyping experiment was conducted to characterise and compare the RSAs of the three species.

Phenotypic measurements are summarized in Table 2. Cucurbit displayed the widest range of root diameters, producing both the thickest (1.67 mm) and the finest (0.139 mm) roots. In contrast, pepper exhibited a narrower diameter range, with apical diameters between 0.204 and 0.98 mm. Branching dominance—reflecting the hierarchical contrast between mother and daughter roots—was highest in squash (0.237), compared with tomato (0.261) and pepper (0.269). Squash also produced more widely spaced lateral roots (3.18 mm) than tomato (2.49 mm) and pepper (2.63 mm). Regarding growth dynamics, root elongation rate and lateral root emission were nearly twice as high in tomato and squash as in pepper.

These traits were used to calibrate the 3D RSA model ArchiSimple (Pagès et al., 2014), enabling us to simulate healthy root architectures at 30 days after sowing (DAS, inoculation date) and 70 DAS (completion of the first nematode cycle). Model outputs (Fig. 5) highlighted pronounced species differences. Cucurbit consistently developed the deepest root system owing to rapid axial elongation and low branching density. By 30 DAS, the primary root had already reached ~80 cm depth, compared with 40 cm in tomato and ~20 cm in pepper. By 70 DAS, squash roots extended beyond 2 m and formed a dense, compact architecture. Pepper showed the shallowest and least extensive root system: although root depth reached ~50 cm at 70 DAS, most lateral roots remained concentrated within the top 20 cm due to limited elongation and low adventitious root production. Tomato displayed an intermediate RSA, characterised by uniform soil exploration down to ~60 cm and abundant thin, highly branched secondary roots.

	Minimal apical diameter (mm)	Apical diameter for order 1 (mm)	Inter-branch distance (mm)	Branching dominance	Rate of adventitious root emission (jour⁻¹)	Potential elongation rate (mm.mm⁻¹.jour⁻¹)
<i>Tomate</i>	0.171	0.99	2.49	0.261	1,9	23.5
<i>Pepper</i>	0.204	0.98	2.63	0.269	1,2	10.7
<i>Cucurbit</i>	0.139	1.67	3.18	0.237	0,8	22.8

Table 1 : Main traits of the root system architecture obtained by the root phenotyping experiment.

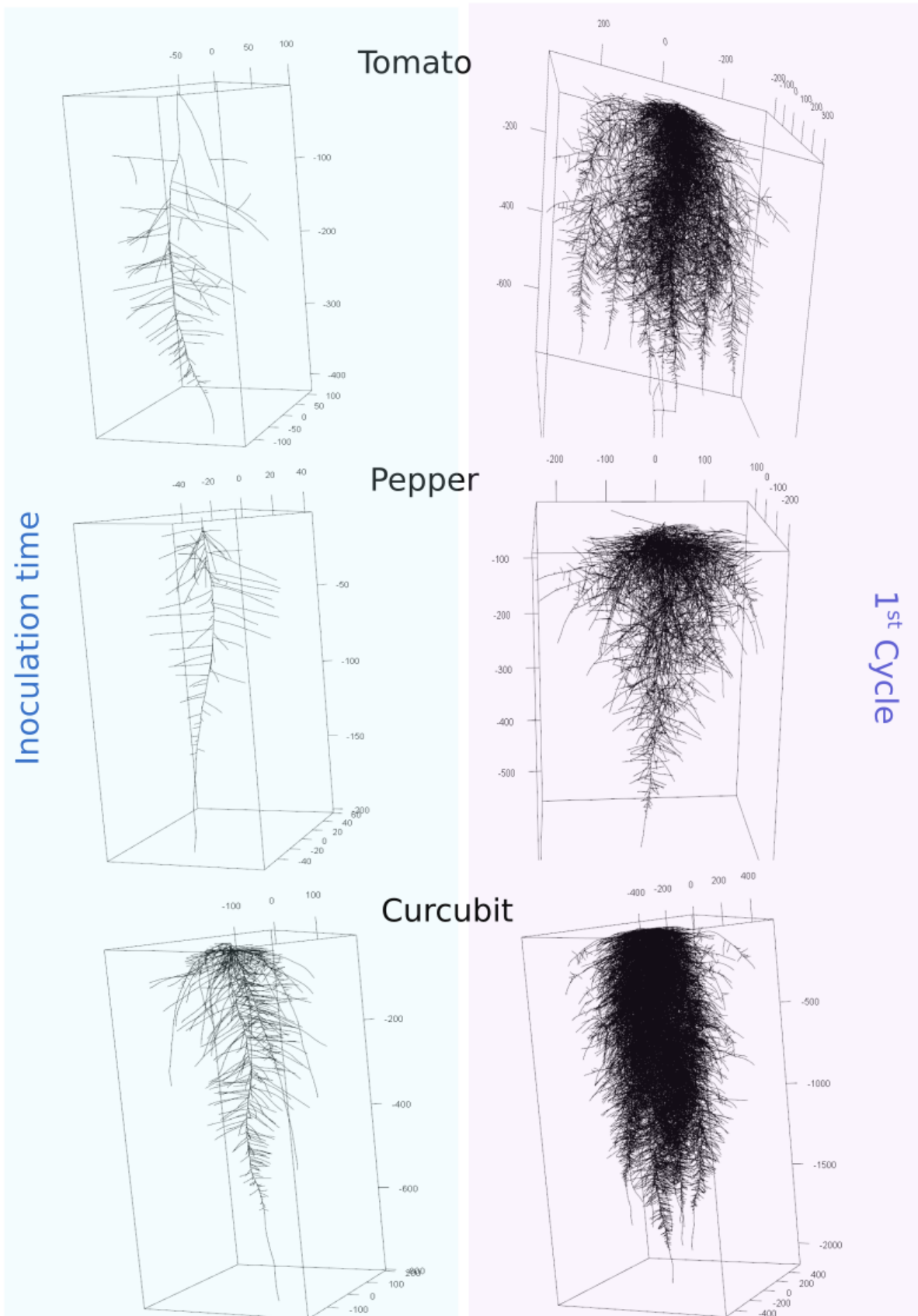


Figure 5 : Root system architecture predicted by the ArchiSimple model (Pages et al. 2014) respectively at 30 DAS (inoculation time) and 70 DAS (first nematode cycle), for the three species.

Root hydraulic conductance and nematode effect

To assess how *M. incognita* affects water transport, we quantified hydraulic properties of the three species under control and inoculated conditions, at two time points, and normalized values by root biomass to account for growth differences.

Cucurbit exhibited the highest hydraulic conductance, both at the level of the single root segment and of the total root system. Tomato and pepper showed comparable conductance. As expected, hydraulic conductance increased with root diameter and biomass but the exact relationship showed species-specific patterns. In particular, the slope was stronger for cucurbit, followed by tomato and then pepper, in agreement with the higher root elongation rate and diameters observed in the phenotyping experiment.

Nematode-induced galls are known to disrupt vascular continuity and divert water and nutrients toward the developing parasite (Bartlem et al. 2016).

Measurements on infected root segments confirmed a localised reduction in axial conductivity in the presence of galls. Thin roots, up to 1mm-diameter were the most affected; but root growth and formation of new xylem vessels progressively offset the impact of nematode and help restore water transport (Figure 6).

Species differed in their sensitivity to nematode-induced hydraulic impairment. At equivalent, small root sections, tomato experienced the greatest reduction in axial conductance, with a six-fold decrease relative to the control case, followed by pepper. In contrast, cucurbits showed no significant difference in axial conductance between control and infected root segments. At the whole plant scale, total hydraulic conductance remained unaffected (p -values $>0,05$) across species at this early stage (2–3 weeks post-inoculation), consistent with the relatively low infection intensity (Figure S1). The hydraulic impact of *M. incognita* is expected to intensify in subsequent nematode cycles as galls expand and reinfection accumulates on older root segments.

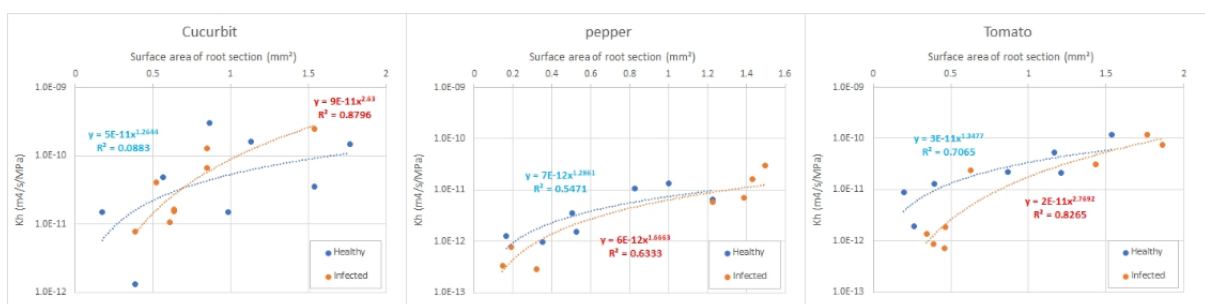


Figure 6: Measured hydraulic conductance of healthy and infected root segments, as a function of root size. The data show that the presence of galls impairs the hydraulic conductance of small roots, especially in tomato.

Species photosynthetic efficiency and CO2 response

Carbon assimilation is a key resource sustaining nematode feeding and gall development. Because RKN infection is known to affect photosynthesis, —through stomatal closure, reduced hormone transport or decreased chlorophyll content (Loveys & Bird 1973, Galvez et al. 2019) —the

intrinsic photosynthetic performance of each species may influence both infection dynamics and host tolerance.

To evaluate these differences, photosynthetic responses were measured under controlled conditions across a wide range of CO₂ concentrations in healthy plants. The data were fitted according to the method of Long and Bernacchi (2003) allowing inference of limiting steps and estimation of biochemical parameters (see Methods and Materials). Estimated values are reported in Table 2.

Across all three species, photosynthesis was Rubisco-limited under low to intermediate CO₂ concentrations. At higher CO₂, assimilation became limited by RuBP regeneration. However, biochemical parameter differences were observed among the species and leaves. In particular, two distinct behaviours were detected in pepper: older leaves had a rapid saturation of the photosynthetic rate compared to younger leaves, which showed continuously increasing photosynthesis with CO₂ levels (see Figure S2). To improve the quality of parameter estimation, we decided to analyse the data for the two age classes separately.

The highest photosynthetic rates were obtained in cucurbits and in young pepper leaves. The two species indeed exhibited similar Rubisco activities and dark respiration rates, but pepper showed a higher electron transport rate (J₆₀₀), indicating a reduced RuBP limitation compared to cucurbit.

Tomato exhibited a lower photosynthetic rate than the other species in both the Rubisco- and RuBP-limiting regimes. Indeed, Rubisco activity was 40% lower in tomato than in cucurbits and peppers, whereas J₆₀₀ showed a 20% reduction. No evidence of TPU limitation was detected within the tested CO₂ range, for any species.

The results of ACI fitting are consistent with the water use efficiency of the species, i.e. the net CO₂ assimilation per unit of water loss, which is often linked to the species' drought tolerance strategy. Accordingly, pepper (young leaves) had the highest WUE, followed by cucurbit and tomato. The low water use efficiency of tomato plants in particular suggests a higher sensitivity to water-stressed conditions, such as those induced by RKN.

Species	V_{max}	R_d	J₆₀₀
Cucurbit	133.1 ± 3.7	6.9±0,5	115,6±3,2
Pepper -old leaves	121,5 ± 6,6	6,3±0,9	105,6±5,8
Pepper -young leaves	133,7±2,3	6,06±0,38	128,3±2,2
Tomato	80,5 ±3,8	1,5±0,9	96,8±4,6

Table 2: Estimated photosynthetic parameters.

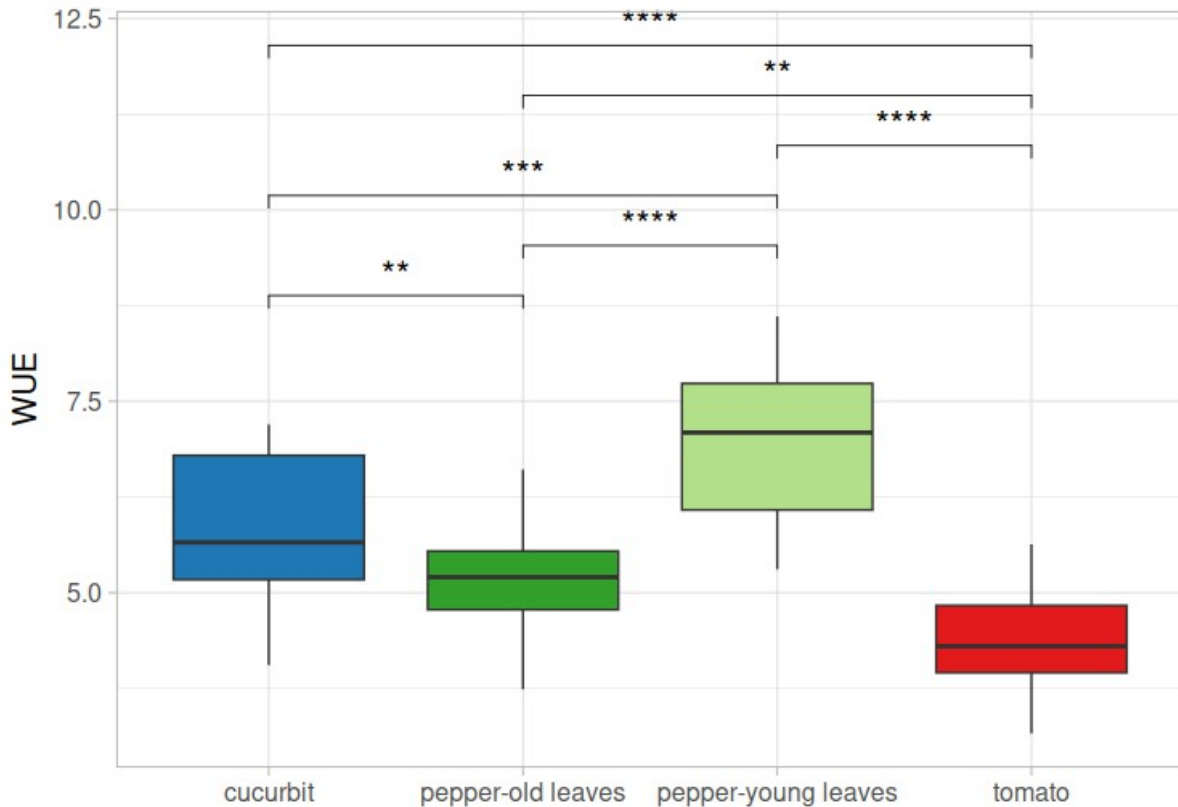


Figure 7: Water use efficiency (WUE) calculated for the three species, over the RuBP-limiting phase.

Discussion

Given that tolerance refers to a plant's capacity to endure or minimize the damage generated by nematode infection, elucidating the relationships between the underlying mechanisms of damage and the resulting yield losses is essential for a comprehensive understanding of tolerance processes. According to Trudgill (1991), root-feeding nematodes may reduce plant growth through several potential mechanisms: (a) direct parasitic effects, involving the withdrawal of approximately 5–15% of the plant's nutrients by developing females of endoparasitic species such as RKN (Melakeberhan & Ferris, 1989); (b) mechanical or physiological impairment, resulting from gall formation that disrupts xylem integrity (Meon et al., 1976) and consequently diminishes water uptake (Wilcox-Lee & Loria, 1987); and (c) systemic physiological effects, including substantial reductions in leaf photosynthetic rate per unit area (Loveys & Bird, 1973), which directly limit shoot growth or alter assimilation, respiration, dry matter allocation, and other metabolic activities.

In the present study, we analysed these parameters in three plant species, tomato, pepper, and cucurbit, to identify potential correlations with their tolerance to *Meloidogyne incognita* and marked species-specific differences in the susceptibility, tolerance, and physiological responses of crops to *Meloidogyne incognita*. By combining RKN infection monitoring, plant phenotyping, hydraulic measurements, and root system modelling, we provide an integrated understanding of how host traits shape the dynamics of RKN infestation and the resulting impact on plant performance.

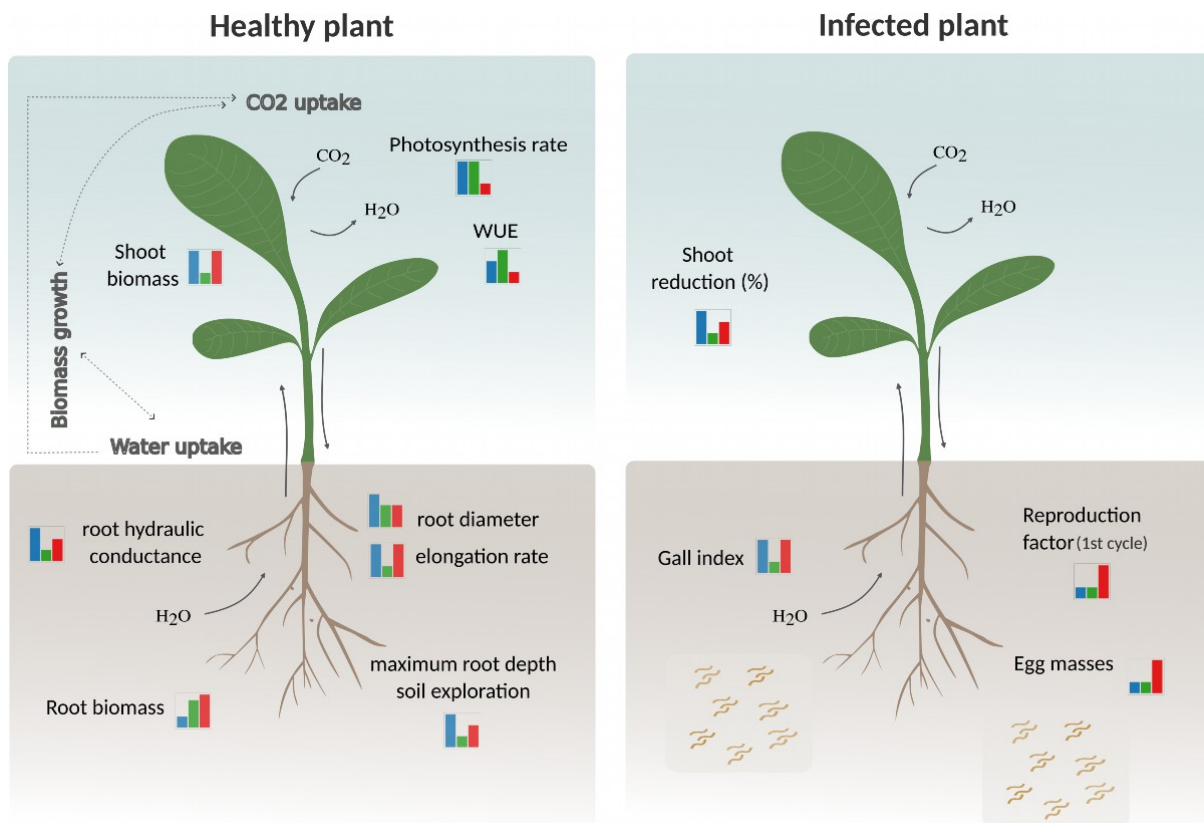


Figure 8: Schematic representation of measured differences between cucurbit (blue bars), pepper (green bars) and tomato (red bars). Left: differences in plant physiological and architectural traits . Right: Differences in the observed infection dynamics.

The progression of nematode infection differed significantly among the three plant species, confirming that host suitability results from the interaction between the nematode and root traits (Trudgill & Blok, 2001; Perry et al., 2009). **Tomato** behaved as a highly favourable typical host, with rapid establishment and high reproduction during the first cycle, consistent with previous observations of the high compatibility of *M. incognita* with solanaceous crops (Sasser & Carter, 1985). The subsequent decrease in the Pf/Pi ratio suggests a progressive reduction in host suitability, possibly related to the activation of induced defences (Shukla et al., 2018) or to the degradation of gall quality (Gheysen & Mitchum, 2019). Conversely, **pepper** exhibited a delayed but subsequently accelerating infection, a pattern consistent with reduced initial penetration due to their compact root system (Prot & Van Gundy, 1981), combined with an ability to maintain essential root functions despite infection. **Cucurbit** exhibited the most severe and high root gall index, consistent with their classification as highly susceptible hosts (Ploeg & Fernandez, 2020). Juvenile densities in the soil corroborate these infection profiles, indicating a greater accumulation of nematodes in tomato and cucurbits than in peppers—a major determinant of the severity of long-term field damage (Karszen et al., 2013).

The growth reduction observed in tomato and cucurbit after two nematode cycles is consistent with the known cumulative effect of galls on root function, nutrient uptake, and carbon allocation (Melillo et al., 2014). The absence of marked effects after a single cycle confirms that early infections do not immediately result in aerial stress, consistent with studies showing that water and nutrient limitations emerge gradually (Baum et al., 2019). The pepper maintained stable growth despite increased nematode reproduction, illustrating a tolerance strategy in which the plant preserves its functions despite a moderate level of infection (Roberts, 2002).

Di Vito et al. (1991) and Seid et al. (2015) reported that infestations by *Meloidogyne* spp. in susceptible **tomatoes** can result in yield losses ranging from 30% to 100%, depending on the initial soil inoculum density, which may vary between 0.03 and 32 eggs or second-stage juveniles (J2) per cm³ of soil (Di Vito et al., 1991; Seid et al., 2015). Several studies have documented severe yield reductions under high infestation pressure, including losses of up to 80% in Anatolia, Turkey (Kaskavalci, 2007).

Di Vito et al. (1985) and Moosavi & Branch (2015) demonstrated that, despite the relatively lower susceptibility of **pepper** (*Capsicum annuum*), yield losses are positively correlated with the initial soil inoculum density. Losses of 40–50% have been reported at initial population densities (Pi) of 8–9 eggs and second-stage juveniles (J2) per cm³ of soil, with maximum yield reductions reaching up to 88% at the highest infestation levels (Pi = 812 eggs or J2 per cm³ of soil) (Di Vito et al., 1985; Moosavi & Branch, 2015). Similarly, Lindsey et al. (1982) reported that *Meloidogyne incognita* densities as low as 0.1–1 eggs and J2 per cm³ of soil significantly restricted the growth of several pepper cultivars after 120–150 days of cultivation (corresponding to 16–21 WAI). Di Vito et al. (1985) corroborated these findings, noting, however, that visible symptoms were not apparent at inoculum levels below 16 nematodes per cm³ of soil. In the present study, we used an initial inoculum (Pi) of 10 nematodes per cm³ of soil and observed no significant effect on pepper growth at 12 WAI, which is consistent with these earlier reports.

According to Trudgill (1991), using the equation developed by Seinhorst (1965) based on Nicholson's competition model (Nicholson, 1933), when a plant sustains several nematode generations, a progressive increase in Pi can occur. This increase tends to be greater in tolerant genotypes than in susceptible ones—a phenomenon that may obscure initial differences in tolerance, as observed in pepper after two *M. incognita* life cycles in our study.

For **cucurbits**, melon (*Cucumis melo*), watermelon (*Citrullus lanatus*), and cucumber (*Cucumis sativus*), experimental studies have shown that yield losses begin to occur at initial population densities (Pi) as low as 0.2 eggs or J2 of *M. incognita* per cm³ of soil, reaching approximately 65% yield reduction at Pi > 0.3 and complete (100%) yield loss at Pi = 16 (Di Vito et al., 1983; Philipps, 2001; Xing & Westphal, 2012; Giné et al., 2014). Field trials on zucchini (*Cucurbita pepo*) reported yield reductions of 39% in spring cropping cycles and 31% in autumn, corresponding to Pi values of 0.03 and 0.006 eggs or J2 per cm³ of soil, respectively (Vela et al., 2014). Given their pronounced susceptibility to RKN, cucurbits are commonly grafted onto tolerant interspecific hybrid squash rootstocks (*Cucurbita moschata* × *C. maxima*) (Collange, 2011; El-Wanis et al., 2013; Ayala-Donas et al., 2020). These rootstocks exhibit a markedly lower number of root galls, females, and egg masses compared with other cucurbits. Moreover, grafting onto such tolerant hybrids has been shown to significantly enhance yield, fruit quality traits, and chlorophyll content relative to non-grafted cucurbits (El-Wanis et al., 2013). In our experiment using this tolerant rootstock and an initial inoculum density (Pi) of 10 nematodes per cm³ of soil, the cucurbit plants were, contrary to expectations, severely affected by nematode infestation.

Exploring species architectural and physiological traits provided clues to the observed tolerance expression. Root system phenotyping and modelling showed that cucurbits are characterised by thick roots, and a fast elongation rate which can give rise to a dense and deep root system. The observed root diameters and depths of different cucurbit accessions, commonly used a rootstocks, align with our estimations (Bertucci et al 2018). The two *Solanaceae*, on the other hand, had thinner roots and explored the soil less deeply. Pepper, in particular, had a very slow elongation rate, whereas tomato developed laterally thanks to the high emission of secondary roots. The measured

values are consistent with those reported by Bui et al. (2015) for several *Solanaceae* genotypes in terms of root diameter, branching density and adventitious root emission. However, the measured elongation rate for pepper was slightly lower than expected.

Root architecture is an important agronomic trait, that is strongly linked to plant growth, yield and abiotic stress tolerance. Under water stress conditions, like the one induced by RKN infection, total root length, maximum root depth and lateral roots development have been pointed out as key ingredients for a good water use efficiency (Tron et al. 2015, Guo et al. 2024).

Rapid root growth and lateral root development have also been associated to increased tolerance to cyst nematodes, in potato (Trudgill & Cotes, 1983, Villordon, A. & Clark, C. (2018) Moreover, several studies have shown that population densities of RKN decrease with soil depth, with the highest abundance occurring in the top 40–60 cm of soil (Wesemal et al., 2008; Ogbuji et al., 1981; Rodriguez-Kabana & Robertson, 1987).

Therefore, in field conditions, a deep root system architecture such as that of cucurbits, can act as an escape mechanism, allowing the plant to quickly access wet, poorly-infested soil layers. In combination with large xylem vessels, this may enable cucurbits to maintain sufficient water uptake and transport despite RKN infestation, as demonstrated by measurements of the hydraulic conductivity of infected root segments. However, pot culture (2L pots, 20 cm deep) severely restricted root development in our plant growth experiment, preventing the expression of such traits and cancelling out their potential advantages.

Root system architecture is not the only factor affecting plant's response to RKN though. In fact, despite having a small, slow-growing root system, pepper plants were more tolerant than the tomato plants. Analysis of photosynthesis in the plants revealed that, like cucurbits, pepper plants had a high photosynthetic capacity in terms of both Rubisco activity (V_{max}) and electron transport chain activity (J_{600}). The latter is particularly important under water-stressed conditions, as these directly affect the concentration of ATP synthase and RuBP synthesis (Tezara et al., 199). Consequently, pepper plants can sustain plant growth by providing high CO_2 assimilation rates despite carbon diversion by RKN and hydraulic impairment. In contrast, tomato plants exhibited low photosynthesis rates and poor water use efficiency, which may partly explain the severe symptoms observed. Consistent with this observation, Melakeberhan et al. demonstrated that the translocation of photosynthate to feeding sites was greater in susceptible than tolerant grape cultivars, despite lower total CO_2 assimilation (Melakeberhan et al., 1990).

The above results demonstrate that plant tolerance is a complex trait resulting from the interaction of multiple physiological and architectural mechanisms at shoot and root levels (see Figure 8). Furthermore, different species can establish distinct tolerance strategies, the efficiency of which is contingent on the local environmental or management conditions.

Previous studies and ours indeed demonstrated that differences in plant tolerance are generally not discernible under controlled pot conditions (Cook & Evans, 1987) and therefore require evaluation under field conditions. This necessity considerably increases the complexity of assessing genotypic responses to nematode infection. Consequently, elucidating the nature and function of tolerance-related traits and the development of a mathematical model linking the different parameters of infestation and plant physiology are of paramount importance, both for the advancement of plant breeding programs and for the development and refinement of integrated management strategies aimed at mitigating root-knot nematode (RKN) soil infestations.

The development of a rapid, non-destructive method for detecting plant infections caused by root-knot nematodes using portable UV-VIS-NIR spectroscopy is currently in progress. This technology enables non-invasive measurements of mineral elements and pH/redox at the leaf level. The device

will make it possible to perform foliar analyses on both infected and healthy plants and to relate variations in mineral concentrations observed in root galls to the overall physiology of the plant. When combined with generative artificial intelligence, it will allow real-time data interpretation and propose potential explanations for observed deviations. If proven effective, this new tolerance indicator will complement the findings presented in this study and could serve as a valuable tool for plant breeders.

Contributions

NJ-G. collected and analysed data on plant growth and RKN development. C.C. helped in plant culture and provided technical assistance. L.P, V.S and C.D conducted the root phenotyping experiment. C.D performed hydraulic measurements and ran simulations with the ArchiSimple model. P.F and S. J. carried out root microscopy and image analysis. VB and S.T. conducted A/Ci measurements and related statistical analysis. V.B and C.D-C. conceived the study and supervised the project. V.B., and C.D-C. wrote the paper with input from all authors. All authors approved the final manuscript.

Acknowledgments

Anne-Violette Lavoit for help and advices in photosynthesis measurements. Joseph Penlap Tamagoua, Cécile Bresch for help in experiments.

References

- Abd-Elgawad, M.M.M., 2014. Yield losses by phytonematodes: challenges and opportunities with special reference to Egypt. *Egyptian Journal of Agronomy* 13(1): 75-94.
- Ayala-Doñas A, Cara-García Md, Talavera-Rubia M, Verdejo-Lucas S. Management of Soil-Borne Fungi and Root-Knot Nematodes in Cucurbits through Breeding for Resistance and Grafting. *Agronomy*. 2020; 10(11):1641. <https://doi.org/10.3390/agronomy10111641>
- Barbary A., Djian-Caporalino C., Palloix A., Castagnone-Sereno P., 2015. Mini-review: Host genetic resistance to root-knot nematodes, *Meloidogyne* spp., in Solanaceae: from genes to the field. *Pest Manag Sci*. 71, , 1591–1598. DOI 10.1002/ps.4091.
- Baxter I, Hosmani PS, Rus A, Lahner B, Borevitz JO, Muthukumar B, et al. (2009) Root Suberin Forms an Extracellular Barrier That Affects Water Relations and Mineral Nutrition in Arabidopsis. *PLoS Genet* 5(5): e1000492. <https://doi.org/10.1371/journal.pgen.1000492>
- Bernacchi, C. J. and Singaas, E. L. and Pimentel, C. and Portis Jr, A. R. and Long, S. P (2001) Improved temperature response functions for models of {Rubisco}-limited photosynthesis. *Plant, Cell & Environment*, 24:253--259
- Bernard, G. C., Egnin, M., and Bonsi, C. (2017). The impact of plant-parasitic nematodes on agriculture and methods of control. *Nematology-concepts diagnosis control* 1, 121–151. Doi: 10.5772/intechopen.68958
- Bertucci, M. B., Suchoff, D. H., Jennings, K. M., Monks, D. W., Gunter, C. C., Schultheis, J. R., & Louws, F. J. (2018). Comparison of Root System Morphology of Cucurbit Rootstocks for Use in Watermelon Grafting. *HortTechnology*, 28(5), 629–636. <https://doi.org/10.21273/HORTTECH04098-18>
- Bui H.H., Serra V.,and Pagès L.. 2015. Root system development and architecture in various genotypes of the Solanaceae family. *Botany*. 93(8): 465-474. <https://doi.org/10.1139/cjb-2015-0008>
- Burnham, Kenneth P., et David Raymond Anderson. Model selection and multimodel inference : a practical information-theoretic approach. New York: Springer, 2002.

- Chandra, P.; Sao, R.; Gautam, S.K.; Poddar, A.N. 2010 Initial population density and its effect on the pathogenic potential and population growth of the root knot nematode *Meloidogyne incognita* in four species of cucurbits. *Asian J. Plant Pathol.* 4, 1–15.
- Di Vito M., Cianciotta V., & Zaccheo G. (1991). The effect of population densities of *Meloidogyne incognita* on yield of susceptible and resistant tomato. *Nematol Mediter* 19: 265-268.
- Di Vito, M., Greco N., & Carella A. (1983). The effects of population densities of *Meloidogyne incognita* on the yield of cantaloupe and tobacco. *Nematol Mediter* 11: 169-174.
- Di Vito M., Greco N. & Carella A. (1985) Population Densities of *Meloidogyne incognita* and Yield of *Capsicum annuum*. *J Nematol* 17 (1): 45-49.
- Djian-Caporalino C., 2012. Root-knot nematodes (*Meloidogyne* spp.), a growing problem in French vegetable crops. *EPPO Bulletin* 42 (1): 127-137.
- Elnahal, A. S., El-Saadony, M. T., Saad, A. M., Desoky, E. S. M., El-Tahan, A. M., Rady, M. M., et al. (2022). The use of microbial inoculants for biological control, plant growth promotion, and sustainable agriculture: a review. *Eur. J. Plant Pathol.* 162, 759–792. Doi: 10.1007/s10658-021-02393-7
- El-Wanis, A.B.D.; Mona, M.; Amin, A.W.; Abdel Rahman, T.G. 2013 Evaluation of some cucurbitaceous rootstocks 2-effect of cucumber grafting using some rootstocks on growth, yield and its relation with root-knot nematode *Meloidogyne incognita* and Fusarium wilt, infection. *Egypt. J. Agric. Res.* 91, 235–257.
- Fan, M.; Li, J.; Dai, K.; Liu, M.; Zhou, W.; Zhang, L.; Lin, 2023 S. Root-Knot Density as a New Index Can Quantitatively Diagnose the Damage of Root Nematodes to Plant Growth. *Agronomy* 13, 136. <https://doi.org/10.3390/agronomy13010136>
- Farquhar, Graham D, S. von Caemmerer, et J. A. Berry. (1980)« A biochemical model of photosynthetic CO₂ assimilation in leaves of C3 species ». *Planta* 90, 1: 78-90. <https://doi.org/10.1007/BF00386231>.
- Gálvez A., del Amor F.M. Ros C. López-Marín J. 2019 New traits to identify physiological responses induced by different rootstocks after root-knot nematode inoculation (*Meloidogyne incognita*) in sweet pepper. *Crop Protection*, 119, 126-133
- Giné A, López-Gómez M, Vela MD, Ornat C, Talavera M, Verdejo-Lucas S, et al., (2014) Thermal requirements and population dynamics of root-knot nematodes on cucumber and yield losses under protected cultivation, *Plant Pathol* 63:1446–1453 .
- Guo C., Bao X., Sun, H., Zhu L., Zhang Y., Zhang K., Bai Z., Zhu J., Liu X., Li A., Dong H., Zhan L., Liu L., Li C., Optimizing root system architecture to improve cotton drought tolerance and minimize yield loss during mild drought stress, *Field Crops Research*, 308,2024,109305
- Jones J, Gheysen G., and Fenoll C. (Eds), 2011. *Genomics and Molecular Genetics of Plant-Nematode Interactions*. Springer, ISBN 978-94-007-0433-6
- Jones J.T, Haegeman A., Danchin E.G.J., Gaur H.S., Helder J., Jones M.G.K, Kikuchi T., Manzanilla-López R., Palomares-Rius J.E., Wesemael W.M.L. and Perry R.N., 2013. Top 10 plant-parasitic nematodes in molecular plant pathology. *Molecular Plant Pathology* 14, 946–961. DOI: 10.1111/mpp.12057.
- Kaskavalci G. (2007) "Effects of Soil Solarization and Organic Amendment Treatments for Controlling *Meloidogyne incognita* in Tomato Cultivars in Western Anatolia," *Turkish Journal of Agriculture and Forestry*: Vol. 31: No. 3, Article 3. Doi: <https://journals.tubitak.gov.tr/agriculture/vol31/iss3/3>
- Long, S. P., et C J Bernacchi. Gas Exchange Measurements, What Can They Tell Us about the Underlying Limitations to Photosynthesis? Procedures and Sources of Error. *Journal of Experimental Botany* 54, nº 392 (2003): 2393-2401. <https://doi.org/10.1093/jxb/erg262>.
- López-Gómez, M.; Flor-Peregrín, E.; Talavera, M.; Sorribas, F.J.; Verdejo-Lucas, S. 2015 Population dynamics of *Meloidogyne javanica* and its relationship with the leaf chlorophyll content in zucchini. *Crop Prot.* 70, 8–14.
- Loveys, B.R. and Bird, A. F. 1973 The influence of nematodes on photosynthesis in tomato plants. *Physiological Plant Pathology*, 4, 525--529
- Maqbool M.A. & Kerry B., 1997. Plant nematode problems and their control in the Near East Region. *FAO Plant Production and Protection Paper* 144.
- Mateille T., 1994. Biologie de la relation plantes-nématodes: Perturbations physiologiques et mécanismes de défense des plantes, *Nematologica* 40:276–311.
- Maurel, C., Nacry, P. Root architecture and hydraulics converge for acclimation to changing water availability. *Nat. Plants* 6, 744–749 (2020). <https://doi.org/10.1038/s41477-020-0684-5>
- Melakeberhan H, Ferris H, Dias JM. Physiological Response of Resistant and Susceptible *Vitis vinifera* Cultivars to *Meloidogyne incognita*. *J Nematol.* 1990 Apr;22(2):224-30

- MBTOC, 2006. *Report of the Methyl Bromide Technical Options Committee. Non-chemical Alternatives Adopted as Replacements to Methyl Bromide on a Large Scale*, pp. 39–73. United Nation Environmental Programme, UNON Publishing Section Services, Nairobi (KE).
- Moens M, Perry RN, and Starr JL, 2009. *Meloidogyne species - a diverse group of novel and important plant parasites*, In: Perry R.N., Moens M. and Starr J.L. (eds) *Root-knot Nematodes*, CAB International:1–17. Doi: 10.1079/9781845934927.0001
- Moosavi MR and Branch M, Damage of the root-knot nematode *Meloidogyne javanica* to bell pepper , *Capsicum annuum*, J Plant Dis Prot 122:244–249 (2015).
- Ney, B., Bancal, M.O., Bancal, P. *et al.* Crop architecture and crop tolerance to fungal diseases and insect herbivory. Mechanisms to limit crop losses. *Eur J Plant Pathol* **135**, 561–580 (2013). <https://doi.org/10.1007/s10658-012-0125-z>
- North G. B. and Nobel P. S., 1995, Hydraulic conductivity of concentric root tissues of *Agave deserti* Engelm. under wet and drying conditions. *New Phytologist*, 130, 47–57.
- Ogbuji, R.O. Soil depth distribution of the root-knot nematode (*Meloidogyne incognita*) from two farmlands in a humid tropical environment. *GeoJournal* **5**, 79–80 (1981)
- Okorley, B. A., Agyeman, C., Amisah, N. & Nyaku, S. T. Screening Selected Solanum Plants as Potential Rootstocks for the Management of Root-Knot Nematodes (*Meloidogyne incognita*). *Int. J. Agron.* 2018, 1–9 (2018).
- Ortiz, Paz., R.A., Guzmán Piedrahita, Ó.A., y Leguizamón Caycedo, J. 2015. Manejo integrado del ematode del nudo radical *Meloidogyne incognita* (Kofoid y White) Chitwood y *Meloidogyne mayaguensis* (Rammh y Hirschmann) en almácigos de guayabo (*Psidium guajava* Linneo), variedad Palmira ICA-1. *Boletín Científico. Centro de Museos. Museo de Historia Natural* 19(2):104-138
- Pagès L., Bécel C. , Boukcim H. et al., 2014, Calibration and evaluation of ArchiSimple, a simple model of root system architecture. *Ecological Modelling*, 290, 76-84.
- Ploeg AT and Phillips MS, Damage to melon (*Cucumis melo* L.) cv. Durango by *Meloidogyne incognita* in Southern California, *Nematology* 3:151–157 (2001).
- Seid A, Fininsa C, Mekete T, Decraemer W, and Wesemael WML, Tomato (*Solanum lycopersicum*) and root-knot nematodes (*Meloidogyne* spp.)-a century-old battle, *Nematology* 17:995–1009 (2015).
- Seinhorst JW (1970) Dynamics of population of plant parasitic nematodes. *Annu Rev Phytopathol* 8:131–156
- Shilpa, P.S.; Thakur, V.; Sharma, A.; Rana, R.S.; Kumar, A. A status-quo review on management of root knot nematode in tomato. *J. Hortic. Sci. Biotech.* 2022, 97, 403–416.
- Singh, S. Integrated approach for the management of the root-knot nematode, *Meloidogyne incognita*, on eggplant under field conditions. *Nematology* 2013, 15, 747–757.
- Sorribas F.J., Djian-Caporalino C., Mateille T., 2020. *Nematodes*. Pages 147-174 In: Gullino M., Albajes R., Nicot P. (eds) *Integrated Pest and Disease Management in Greenhouse Crops. Plant Pathology in the 21st Century*, vol 9. Springer, Cham
- Subedi, S., Thapa, B., & Shrestha, J. (2020). Root-knot nematode (*Meloidogyne incognita*) and its management: a review. *Journal of Agriculture and Natural Resources*, 3(2), 21–31. <https://doi.org/10.3126/janr.v3i2.32298>
- Talavera M., Sayadi S., Chirisa-Rios M., Salmeron T., Flor-Peregrin E., Verdejo-Lucas S, 2012. Perception of the impact of root-knot nematode-induced diseases in horticultural protected crops of south-eastern Spain. *Nematology* 14(5), 517-527
- Tezara, W., Mitchell, V., Driscoll, S. *et al.* Water stress inhibits plant photosynthesis by decreasing coupling factor and ATP. *Nature* **401**, 914–917 (1999). <https://doi.org/10.1038/44842>
- Tron S., Bodner G., Laio F., Ridolfi L., Leitner D. (2015) Can diversity in root architecture explain plant water use efficiency? A modeling study, *Ecological Modelling*, Volume 312, 200-210, <https://doi.org/10.1016/j.ecolmodel.2015.05.028>.
- Trudgill D.L , 0066-4286, 29, Resistance to and tolerance of plant parasitic nematodes in plants. *Annual Review of Phytopathology*, 29,167–192, (1991)
- Trudgill, D.L. and Cotes, L.M. (1983), Tolerance of potato to potato cyst nematodes (*Globodera rostochiensis* and *G. pallida*) in relation to the growth and efficiency of the root system. *Annals of Applied Biology*, 102: 385-397. <https://doi.org/10.1111/j.1744-7348.1983.tb02708.x>
- Wesemael W.M.L., Viaene N. & Moens M., 2011. Root-knot nematodes (*Meloidogyne* spp.) in Europe. *Nematology* 13 (1): 3-16.

- Vela MD, Giné A, López-Gómez M, Sorribas FJ, Ornat C, Verdejo-Lucas S, et al., Thermal time requirements of root-knot nematodes on zucchini-squash and population dynamics with associated yield losses on spring and autumn cropping cycles, *Eur J Plant Pathol* 140:481–490 (2014).
- Verdejo-Lucas, S.; Talavera, M. Root-knot nematodes on zucchini (*Cucurbita pepo* subsp. *Pepo*): Pathogenicity and management. *Crop Prot.* 2019, 126, 104943.
- Villordon, A. & Clark, C. Variation in Root Architecture Attributes at the Onset of Storage Root Formation among Resistant and Susceptible Sweetpotato Cultivars Infected with *Meloidogyne incognita*. *HortScience* 53, 1924–1929 (2018).
- Wesemael, W.M.L., Moens, M. Vertical distribution of the plant-parasitic nematode, *Meloidogyne chitwoodi*, under field crops. *Eur J Plant Pathol* 120, 249–257 (2008)
- Xing, L.; Westphal, A. Predicting damage of *Meloidogyne incognita* on watermelon. *J. Nematol.* 2012, 44, 127–133.

Supplementary information

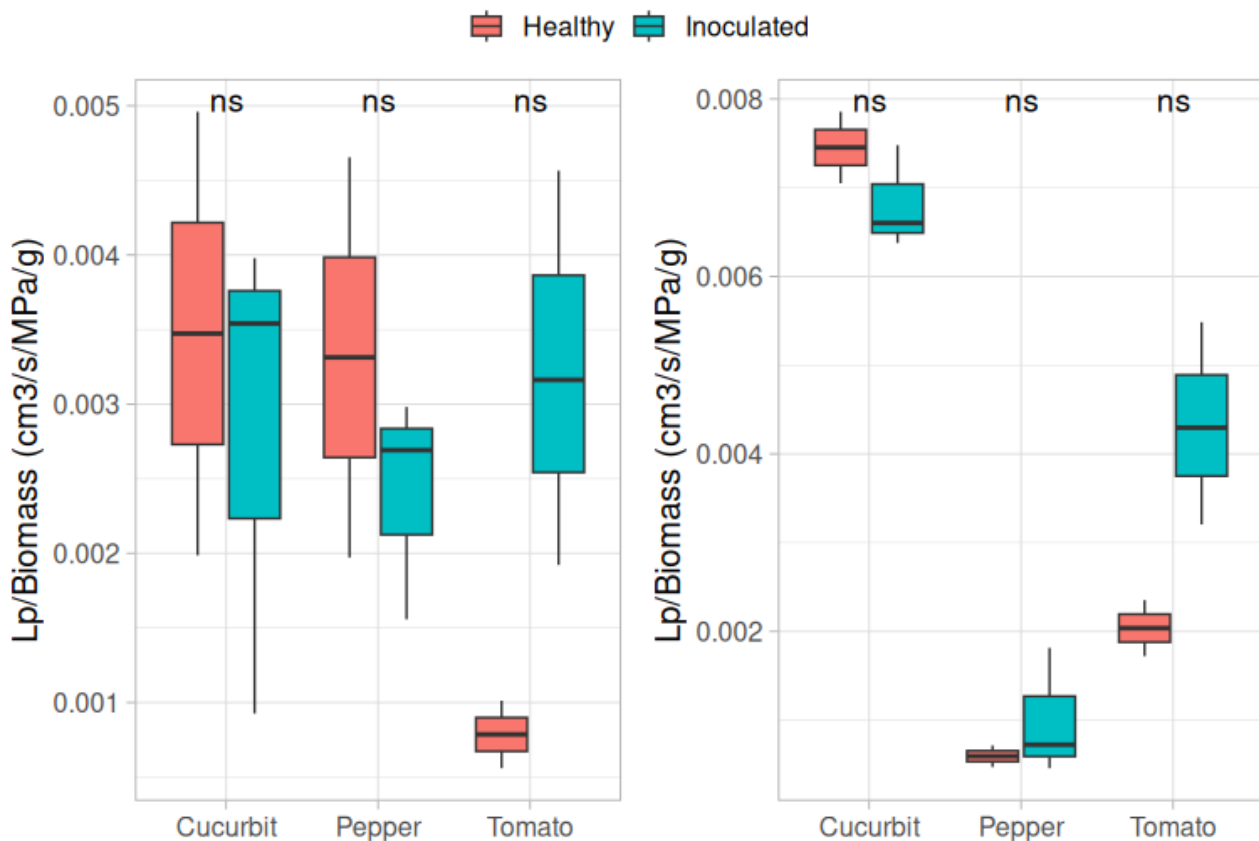


Figure S1: Normalized hydraulic conductance of the whole root system, measured for the three species, in healthy and inoculated conditions. Left: first harvest, between 10 to 20 days after inoculation. Right: second harvest, 20 to 30 days after inoculation.

Parameterization of the ArchiSimple model

The ArchiSimple model, developed by Pages et al., is a generic root architecture model that has been applied to many species. Its strength lies in the parsimony and interpretability of its parameters, which can mostly be inferred directly from experimental data.

Most of the parameters, including the maximal and minimal root tip diameter, have been determined in our phenotyping experiment, as described in M&M. Here after we detail the estimation of the parameters related to adventitious root dynamics as well as the calibration of root lifespan.

Estimation of adventitious roots emission rate

Adventitious roots are secondary root that can originate from non-root organs (stems, nodes..) as a part of developmental program of the plant or as a reponse to wounding or other stressors.

In order to observe the emergence of adventitious roots, the three species were grown in a climate-controlled room for 12 weeks, in 2L pots. Every two weeks, four plants per species were removed from the soil and gently washed under clear water. The number of roots that appeared above the collar and in the first 2 cm of the taproot was counted, assuming that they are mostly adventitious. A linear regression analysis was performed on the data set in order to estimate the time of first emission and the emission rate of each species. Results are reported in Table S1. Linear adjustment was found to be satisfactory for both the tomato and the curcurbit (as indicated by high R^2 values). However, a high degree of variability was observed in pepper, which renders the estimation of this species less reliable.

	Starting emission (day)	Emission rate (day ⁻¹)	Adjusted R ²
Pepper	23,2	1,2±0,4 **	0,28
Tomate	27,3 **	1,9±0,21 ***	0,81
Cucurbit	10,1 .	0,79±0,07 ***	0,87

Table S1: Linear regression estimates for adventitious emission rate and emission time, for the three considered species.

Estimation of root lifespan

The ArchiSimple model assumes that most variation in the architectural and developmental characteristics of plant species can be related to the size of root tip.

Root growth is determined by two factors :growth rate and growth time (or duration), both of which are determined by the apical diameter (d): proportional to d for growth rate and proportional to d^2 for duration. The growth duration coefficient is this coefficient of proportionality to d^2 . After this growth period, the root stops growing and finally starts to necrosis after a delay « Age_max ». The time length Age_max depends linearly on root diameter and the root density , according to a species-specific coefficient called C_life . The root lifespan is then the sum of the growth period and the delay to necrosis.

Root tissue has been fixed 0,1 for tomato and pepper and to 0,08 g/cm³ for curcurbit, based on literature information (Pu et al. 2023, Sallaku et al. 2022). The remaining parameters (C_life, C_growth duration) have been fixed manually by comparing the simulated root architecture to the root biomass measured at 30 and 70 DAS. The resulting values are reported in Table S2.

		Growth phase		Delay before necrosis			Root lifespan	
		d (mm)	C_growth _duration	Growth duration (day)	C_life	Tissue density (g/cm ³)	Age_max (day)	Lifespan (day)
Tomato	min diameter	0,17	75	2,2	150	0,1	2,6	4,7
	max diameter	1		75			15	90
Pepper	min diameter	0,2	450	18	8000	0,1	160	178
	max diameter	1		450			800	1250
Cucurbit	min diameter	0,14	75	1,5	100	0,08	1,1	2,6
	max diameter	1,7		216,8			13,6	230,4

Table S2: Root lifespan and parameters used in the ArchiSimple model.

A-Ci curves fitting

Photosynthesis vs CO₂ curves were fitted following the procedure proposed by Long & Benacchi, 2003, as described in the material & method section. Four to five leaves, from different plants, were measured for each species.

While A-Ci curves were well reproducible for cucurbits, inter-plant variability was high for peppers and tomatoes. To improve the quality of the fit estimation, we decided to separate the leaves according to their age and analyse them separately. Fitted curves are showed in figure S2.

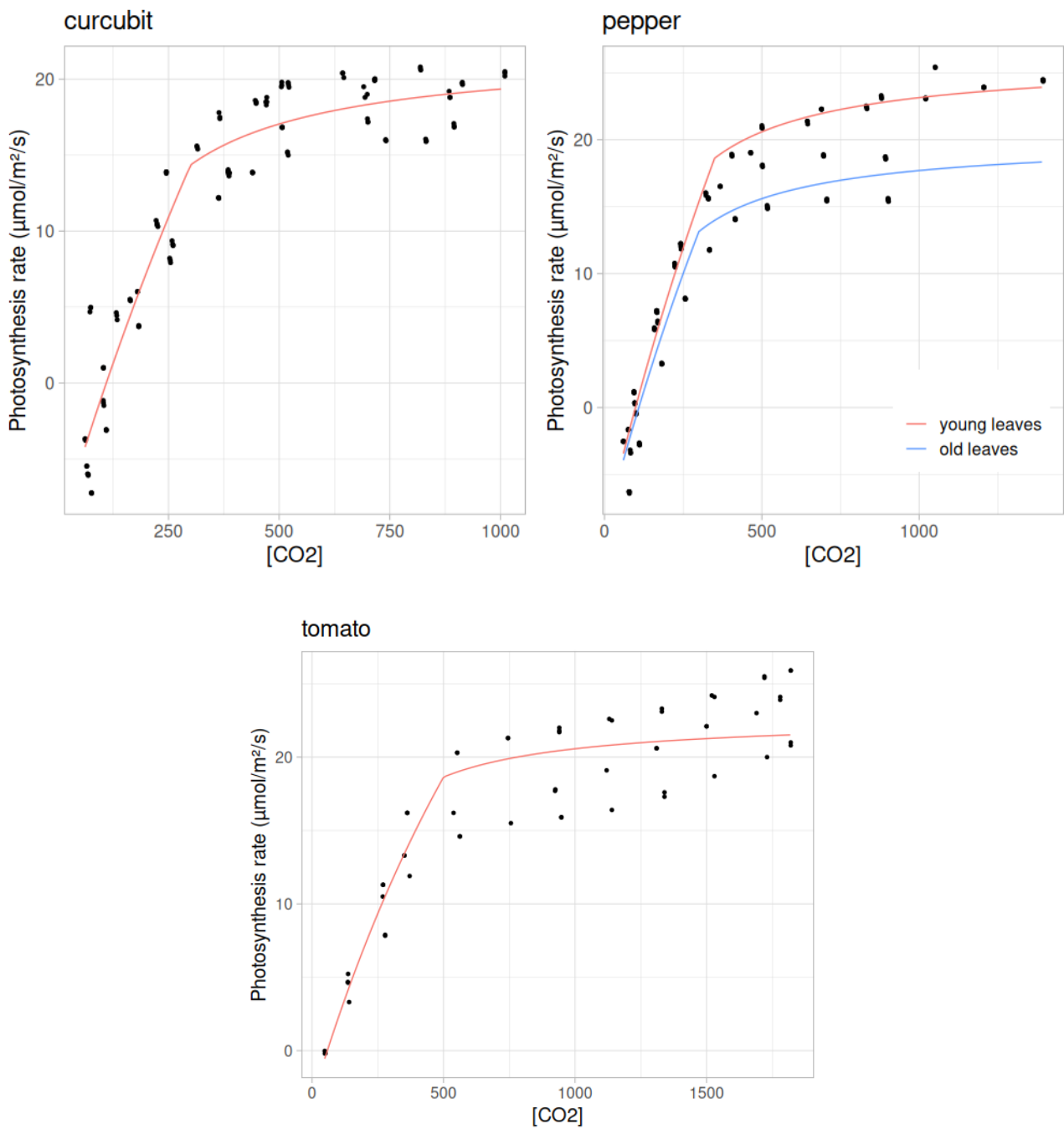


Figure S2 : Courbe fitting of ACI data for the three considered species.

References:

Pu Z., Zhang R. , Wang H., Li Q., Zhang J. , Wang X. Root morphological and physiological traits and arbuscular mycorrhizal fungi shape phosphorus-acquisition strategies of 12 vegetable species, *Frontiers in Plant Science*, 14 (2023).

Sallaku G., Rewald B., Sandén H., Balliu A. Scions impact biomass allocation and root enzymatic activity of rootstocks in grafted melon and watermelon plants, *Frontiers in Plant Science*, 13, (2022).